# A Fast Filtering Proportionate Affine Projection Sign Algorithm

Felix Albu, Henri Coanda
Dept. of Electronics
Valahia University of Targoviste
Targoviste, Romania
e-mail: {felix.albu, coanda}@valahia.ro

***Abstract*—In this paper, a new proportionate affine projection sign algorithm using the $\mu$ -law proportionality idea is proposed. It has an efficient implementation because it uses a fast recursive filtering procedure. Simulation results indicate that the proposed algorithm has slightly better performance than a competing algorithm in a network echo cancellation system in impulsive environments and adaptive feedback cancellation for hearing aids systems.**

***Keywords-Proportionate-type algorithms, adaptive filters, affine projection sign algorithm, fast recursive filtering***

## I. INTRODUCTION

In many practical system identification applications such as network echo cancellation, the echo paths are long and sparse. Adaptive filters are used to identify the echo paths and many adaptive filtering algorithms have been proposed [1]. It is known that the family of affine projection algorithm (APA) [2] has superior performance over the NLMS type of algorithms and multiple applications on echo cancellation and active noise control have been reported (e.g. [3-5]). The proportionate normalized least mean square algorithm (PNLMS) [6] and its improved IPNLMS version [7] exploits the sparseness of the echo paths. An improved algorithm, called the $\mu$ -law PNLMS, used the logarithm of the coefficient magnitudes instead of coefficient magnitudes [8]. The proportionate idea was extended to APA in [9-11]. Another PAPA that uses the $\mu$ -law idea is the $\mu$ -law memory improved PAPA (MMIPAPA) [12]. The MMIPAPA showed further performance improvements over APA/PAPA, but at the cost of additional logarithmic operations [12]. A fast recursive filtering proposed in [13] proved useful in reducing the complexity of the APA and MIPAPA respectively [14]. Also, a version with intermittently weight updating of a PAPA version was proposed in [15].

Unfortunately, the APA and PAPA family of algorithms are not very robust to impulsive noise interference [16], [17]. The robust affine projection sign algorithm (APSA) has been proposed in [16]. The real-coefficient improved proportionate affine projection sign algorithm (RIP-APSA) was presented and proved to be robust to such outliers [18]. Also, other affine projection sign algorithms were proposed in [19-21]. In [18] the RIP-APSA's superiority over APA, APSA and PAPA's in terms of robustness and fast convergence for both sparse and dispersive echo paths in impulsive environments was proved by many simulation results. The logarithmic proportionality principle can be incorporated in the RIP-APSA algorithm and a new algorithm termed $\mu$ -law RIP-APSA (MRIP-APSA) is obtained. Furthermore, the same fast recursive filtering idea is adapted to the MRIP-APSA algorithm and an equivalent implementation is proposed.

The paper is organized as follows. Section II introduces the proposed algorithm and its efficient implementation. The simulation results are presented in Section III for network echo cancellation and adaptive feedback cancellation systems. Finally, Section IV concludes this work.

## II. THE PROPOSED ALGORITHM

The proposed algorithm is derived from the RIP-APSA [18]. The adaptive filter that models the true $L$-length echo path, $\mathbf{h}$, is defined by $\mathbf{w}(k)=\left[w_0(k), w_1(k),..., w_{L-1}(k)\right]^T$, where $k$ is the time index and superscript $T$ denotes transposition. We denotes $x(k)$, $z(k)$ and $v(k)$ as the far-end, the near-end and background noise signals, respectively. The desired signal is $y(k)=\mathbf{x}^T(k)\mathbf{h}+z(k)+v(k)$ where the vector $\mathbf{x}(k)=\left[x(k),...,x(k-L+1)\right]^T$, collects the far-end signal. The output of the adaptive filter is $\hat{y}(k)=\mathbf{x}^T(k)\mathbf{w}(k)$, and the error vector is given as

$$\mathbf{e}(k)=\mathbf{y}(k)-\mathbf{X}^T(k)\mathbf{w}(k), \tag{1}$$

Where $\mathbf{y}(k)=\left[y(k), y(k-1),..., y(k-M+1)\right]^T$, is a $M\times 1$ vector, $M$ is the projection order, and $\mathbf{X}(k)=\left[\mathbf{x}(k), \mathbf{x}(k-1),..., \mathbf{x}(k-M+1)\right]$, is the input signal matrix. The filter coefficients of RIP-APSA [18] are adapted by multiplying the update vector with the proportionate matrix $\mathbf{G}(k)=\text{diag}\{g_0(k),..., g_{L-1}(k)\}$, which contains the proportionate factors, $g_l(k)$ defined as:

$$g_l(k)=\frac{1-\alpha}{2L}+\frac{|w_l(k)|(1+\alpha)}{2\sum_{i=0}^{L-1}|w_i(k)|+\varepsilon},\ l=1..L, \qquad (2)$$

where $-1<\alpha<1$ and $\varepsilon$ is a small positive constant to avoid division by zero [18].

The RIP-APSA computes $\mathbf{x}_{gs}(k)=\mathbf{G}(k)\mathbf{X}(k)\mathrm{sgn}(\mathbf{e}(k))$, where $\mathrm{sgn}(\cdot)$ is the sign function and the weight updating equation for the RIP-APSA is given by the following equation [18]

$$\mathbf{w}(k+1)=\mathbf{w}(k)+\frac{\mu\mathbf{x}_{gs}(k)}{\sqrt{\delta+\mathbf{x}_{gs}^T(k)\mathbf{x}_{gs}(k)}}, \qquad (3)$$

where $\mu$ is the step size and $\delta$ is another small constant to avoid division by zero.

The logarithmic proportionate updating scheme [8], can be incorporated in the RIP-APSA by modifying the proportionate coefficients of (7) as in (10)-(11):

$$g_l(k)=\frac{1-\alpha}{2L}+\frac{|\mathrm{F}(w_l(k))|(1+\alpha)}{2\sum_{i=0}^{L-1}|\mathrm{F}(w_i(k))|+\varepsilon},\ l=1..L, \qquad (4)$$

and $\mathrm{F}(w_l(k))=\ln(1+\mu_l|w_l(k)|)$.where $\mu_l$ is a constant.

Therefore, a new sign algorithm termed the $\mu$-law RIP-APSA (MRIP-APSA) is obtained. The MRIP-APSA requires additional $L$ logarithmic functions and $L$ additions per iteration in comparison with the RIP-APSA. The complexity of the logarithmic function is high, therefore the use of a segmental approximation has been proposed in [8]. However, this approximation is valid only in some limits. In [14] a fast filtering procedure used in [9] has been adapted to the APSA algorithm. The same idea is applied to the MRIP-APSA in order to obtain the efficient implementation of MRIP-APSA.

Substituting (8) into (9) and noting $\mathbf{P}(k)=\mathbf{G}(k)\mathbf{X}(k)$ and $\mathbf{R}(k)=\mathbf{P}^T(k)\mathbf{P}(k)$ leads to

$$\mathbf{w}(k+1)=\mathbf{w}(k)+\frac{\mu\mathbf{P}(k)\mathrm{sgn}(\mathbf{e}(k))}{\sigma(k)}, \qquad (5)$$

where

$$\sigma(k)=\sqrt{\delta+\mathrm{sgn}(\mathbf{e}^T(k))\mathbf{R}(k)\mathrm{sgn}(\mathbf{e}(k))}. \qquad (6)$$

Also we have

$$\begin{aligned}\hat{\mathbf{y}}(k-1)&=\mathbf{X}^T(k-1)\mathbf{w}(k-1)\\&=\left[\mathbf{x}^T(k-1)\mathbf{w}(k-1)..\mathbf{x}^T(k-M)\mathbf{w}(k-1)\right]^T\\&=\left[y^0(k-1)\ y^1(k-1)\ ...\ y^{M-1}(k-1)\right]^T,\end{aligned} \qquad (7)$$

Where $y^n(k-1)=\mathbf{x}^T(k-n-1)\mathbf{w}(k-1)$. Therefore, we obtain:

$$\hat{\mathbf{y}}(k)=\mathbf{X}^T(k)\mathbf{w}(k)=\mathbf{z}(k)+\frac{\mu\mathbf{X}^T(k)\mathbf{H}(k)\mathrm{sgn}(\mathbf{e}(k-1))}{\sqrt{\delta+\mathrm{sgn}(\mathbf{e}^T(k-1))\mathbf{R}(k-1)\mathrm{sgn}(\mathbf{e}(k-1))}} \qquad (8)$$

Where $\mathbf{H}(k)=\mathbf{X}^T(k)\mathbf{P}(k-1)$ and

$$\begin{aligned}\mathbf{z}(k)&=\mathbf{X}^T(k)\mathbf{w}(k-1)\\&=\left[\mathbf{x}^T(k)\mathbf{w}(k-1)..\mathbf{x}^T(k-M+1)\mathbf{w}(k-1)\right]^T\\&=\left[\mathbf{x}^T(k)\mathbf{w}(k-1)\ y^0(k-1)..\ y^{M-2}(k-1)\right]^T\end{aligned} \qquad (9)$$

It can be seen that only $\mathbf{x}^T(k)\mathbf{w}(k-1)$ need to be computed for $\mathbf{z}(k)$ and requires $L$ multiplications and $L-1$ additions. This leads to an important complexity reduction (i.e. from $ML$ multiplications to only $L$ multiplications). Also, only the first row and first column of $\mathbf{H}(k)$ needs to be computed at each iteration. The rest of the matrix elements are the first $M-1$ rows and $M-1$ columns of $\mathbf{H}(k-1)$. The complexity reduction grows linearly with the projection order, $M$. Therefore the fast recursive implementation of MRIP-APSA has the following equations:

Initialization

$$\begin{aligned}&\mathbf{e}(k)=0,\mathbf{w}(k)=0,\mathbf{x}(k)=0,\hat{\mathbf{y}}(k)=0,\\&\sigma(k)=\varepsilon\ \text{ for } k\le 0\end{aligned} \qquad (10)$$

For $k=1,2,...$

$$\mathbf{z}(n)=\begin{bmatrix}\mathbf{x}^T(k)\mathbf{w}(k-1)\ ...\\ y^0(k-1)\ ...\ y^{M-2}(k-1)\end{bmatrix}^T \qquad (11)$$

$$\mathbf{H}(k)=\mathbf{X}^T(k)\mathbf{P}(k-1) \qquad (12)$$

$$\mathbf{q}(k)=\mathbf{H}(k)\operatorname{sgn}\left(\mathbf{e}(k-1)\right) \tag{13}$$

$$\mathbf{g}(k)=\mu\sigma^{-1/2}(k-1)\mathbf{q}(k) \tag{14}$$

$$\mathbf{e}(k)=\mathbf{y}(k)-\hat{\mathbf{y}}(k) \tag{15}$$

$$\hat{\mathbf{y}}(k)=\mathbf{z}(k)+\mathbf{g}(k) \tag{16}$$

$$\mathbf{x}_{gs}(k)=\mathbf{P}(k)\operatorname{sgn}\left(\mathbf{e}(k)\right) \tag{17}$$

$$\mathbf{R}(k)=\mathbf{P}^{T}(k)\mathbf{P}(k) \tag{18}$$

$$\sigma(k)=\sqrt{\delta+\operatorname{sgn}\left(\mathbf{e}^{T}(k)\right)\mathbf{R}(k)\operatorname{sgn}\left(\mathbf{e}(k)\right)} \tag{19}$$

$$\mathbf{w}(k+1)=\mathbf{w}(k)+\mu\sigma^{-1/2}(k)\mathbf{x}_{gs}(k) \tag{20}$$

The MRIP-APSA and its fast recursive implementation are equivalent therefore only MRIP-APSA algorithm results are shown in the next section. Their overall complexity is higher than that of RIP-APSA, especially due to the use of the logarithmic functions. The MRIP-APSA can be integrated in an adaptive feedback cancelation context. More information about these systems can be found in [22]. Suitable algorithms for such systems have been described in [23-24]. In a hearing aid system, the source signal is corrupted by the additive feedback signal generated by the output signal leaking to the input. Also, the hearing-loss has to be considered in order to generate the signals for the adaptive filter. The correspondence with the echo cancellation system signals is the following: the acoustic source signal corresponds to the near-end signal, the feedback signal corresponds to the echo signal, and the output signal corresponds to the far-end signal.

## III. Simulation Results

The RIP-APSA [18], and the MRIP-APSA were simulated in impulsive interference environment and their speed of convergence and tracking abilities were compared. We used $\delta=\varepsilon=0.01$ in the simulations of sign based adaptive algorithms. The input signal was an AR(1) signal with a pole at 0.9. A white noise was added to the near-end signal in order to have a signal-to-noise ratio SNR = 40 dB. The near end signal *z(k)* has a signal-to-interference ratio SIR = 0 dB and is modeled by a Bernoulli-Gaussian (BG) signal [16]. The BG distribution was generated as in [18] as a product of a Bernoulli process with the parameter *Pr* and a Gaussian process, keeping its average power constant. In the impulsive interference environment simulations the value *Pr*=0.002 was used.

The simulations were performed using two network impulse responses (NIR) with $L=512$ coefficients. Their sparseness measure is defined by $\xi=\left(L/L-\sqrt{L}\right)\cdot\left(1-\|\mathbf{h}\|_1/\sqrt{L}\|\mathbf{h}\|_2\right)$, where $0\le\xi\le1$ [25]. The sparse echo path has $\xi=0.758$ and the dispersive echo path has $\xi=0.626$ (see Figure 1). The echo path changed from the sparse NIR to the dispersive NIR after 20000 samples. The performance of the algorithms was measured by the normalized misalignment defined by $\eta(k)=20\cdot\log_{10}\left(\|\mathbf{h}-\mathbf{w}(k)\|_2/\|\mathbf{h}\|_2\right)$, averaged over 10 experiments.

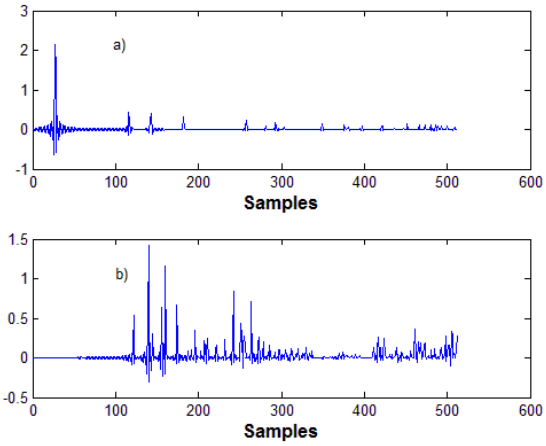


Figure 1: a) The sparse echo path, $\xi=0.758$; b) the dispersive echo path, $\xi=0.626$.

For the first experiment, the convergence and tracking performance of the MRIP-APSA using $\mu=0.01$, $\alpha=0.5$, $M=8$ is shown in Figure 2. Four $\mu_l$ values were used: 1, 10, 100, and 1000. It can be noticed from Figure 2 that the best performance is obtained for $\mu_l=1$. The same conclusion was obtained for other projection orders. This $\mu_l$ value is used in the following simulations.

For the second experiment, the $\alpha$ value is varied, while all the other conditions are the same as for Figure 3. Four $\alpha$ values were used: -1, -0.5, 0, and 0.5. It can be noticed from Figure 3 that the best performance in terms of convergence and tracking abilities is obtained for $\alpha=0.5$. The same conclusion was obtained for other projection orders. This $\alpha$ value is used in the subsequent simulations.

For the third experiment the projection order was varied, while all the other conditions are the same as above. Four *M* values were used: 1 (equivalent to APSA), 2, 4, and 8. It

can be noticed from Figure 4 that the convergence speed increases with an increased projection order value, but the steady-state misalignment increases too. The lowest misalignment for the investigated case is obtained for $M$ = 2.

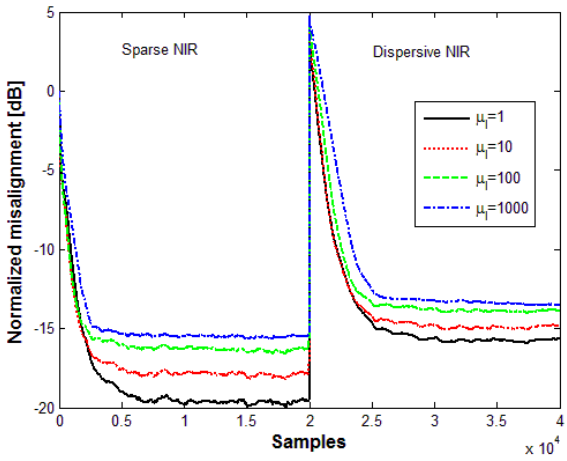


Figure 2: Misalignment of MRIP-APSA with colored input signal and $M = 8$ $\alpha = 0.5$ ,and $\mu = 0.01$ and different $\mu_l$ values.

For the fourth experiment, the convergence and tracking performance of the MRIP-APSA using $\mu_l = 1$, $\alpha = 0.5$, $M = 8$ is shown in Figure 5. Four $\mu$ values were used: 0.01, 0.02, 0.05, and 0.1. It can be noticed from Figure 5 that the convergence speed increases with an increased step size order value, but the steady-state misalignment increases too. This conclusion is valid for both sparse and dispersive echo path.

This conclusion is similar to that obtained for RIP-APSA in [18] that indicates that it is recommended to use $\mu < 0.1$.

For the fifth experiment, the convergence and tracking performance of the MRIP-APSA using $\mu = 0.01$, $\mu_l = 1$, $\alpha = 0.5$, and an under-modeling case.

Only the first 412 coefficients out of the 512 coefficients are used by the adaptive filters that model both the sparse and dispersive NIR channels. Two projection orders were used. By comparing the convergence plots from Figure 4 and Figure 6 in case of $M = 2$ and $M = 8$ it can be noticed that both the under-modeling lead to a reduced convergence speed and higher misalignment values.

This conclusion is also valid for both sparse and dispersive echo path. As expected, the misalignment difference is higher in case of the dispersive echo path. It can be seen in Figure 1 that there are more un-modeled significant coefficients in the last 100 coefficients of the dispersive echo path that in the case of the sparse echo path.

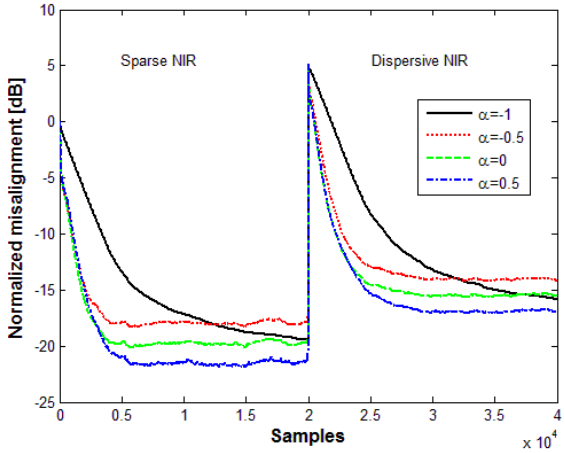


Figure 3: Misalignment of MRIP-APSA with colored input signal, $M = 8$, $\mu_l = 1$, and $\mu = 0.01$ and different $\alpha$ values.

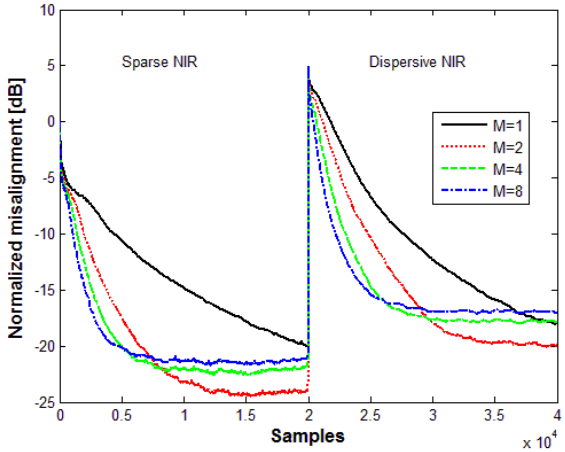


Figure 4: Misalignment of MRIP-APSA with colored input signal, $\mu_l = 1$, $\alpha = 0.5$ and $\mu = 0.01$ and different $M$ values

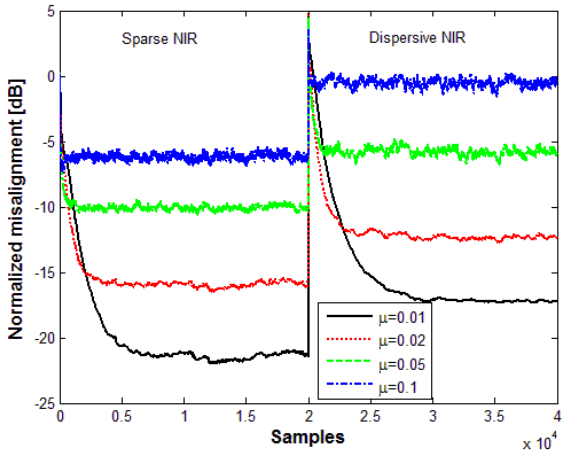


Figure 5: Misalignment of MRIP-APSA with colored input signal, $M = 8$, $\mu_l = 1$, $\alpha = 0.5$, and different $\mu$ values.

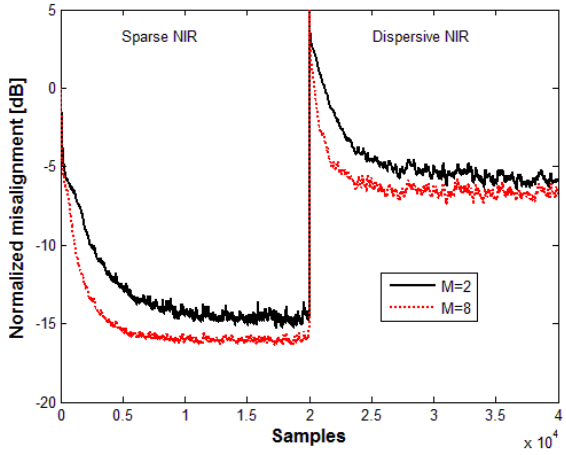


Figure 6: Misalignment of MRIP-APSA with colored input signal, $\mu_l = 1$, $\alpha = 0.5$, $\mu = 0.01$ and two $M$ values for an under-modeling case.

For the sixth experiment, the convergence and tracking performance of the MRIP-APSA and RIP-APSA using $\mu = 0.01$, $\mu_l = 1$, $\alpha = 0.5$ is compared. Two projection orders were used. It can be noticed from Figure 7 that MRIP-APSA can achieve a lower misalignment value than RIP-APSA in case of higher projection value for both sparse and dispersive echo path.

The last simulation investigates the performance of APA, MRIP-APSA and RIP-APSA in the acoustic feedback context. The feedback path was modelled as a finite impulse response filter with 64 coefficients. The adaptive filter had 64 coefficients too. A constant gain of 30 dB in the forward path and a delay of 60 samples were assumed [23]. The sampling frequency was 16 kHz. The other parameters of the algorithms are the same as above.

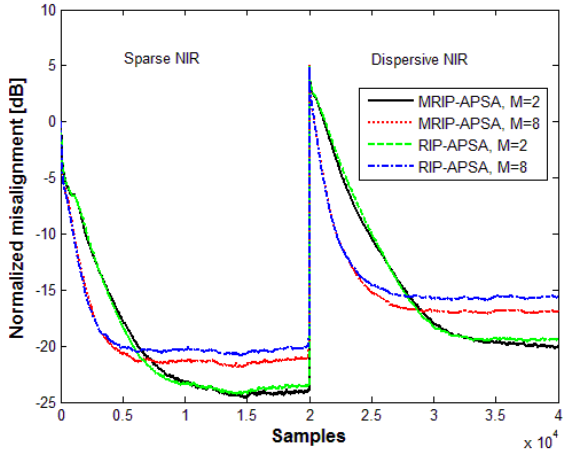


Figure 7: Misalignment of MRIP-APSA and RIP-APSA with colored input signal, $\mu_l = 1$, $\alpha = 0.5$ and $\mu = 0.01$ and different $M$ values.

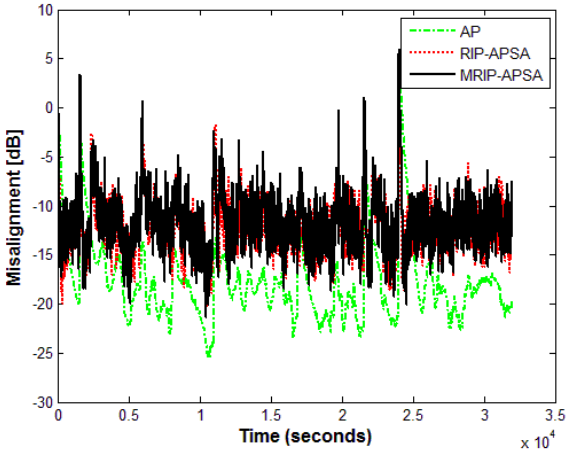


Figure 8. Misalignment of APA, RIP-APSA, and MRIP-APSA for an AFC application with speech input signal, $M = 8$ and $\mu = 0.01$.

It can be seen from Figure 8 that most of the time, the performance of MRIP-APSA is slightly superior to that of RIP-APSA.The AP algorithm obtains a smaller misalignment than the sign based algorithms, although has a slower convergence speed. However, APA has an increased complexity, while the sign based algorithms replaces many of the multiplications with additions. Our future work will be focused on investigating the performance of MRIP-APSA on an AFC application using two microphones in hearing devices [26].

## ACKNOWLEDGMENT

This work was supported by a grant of the Romanian National Authority for Scientific Research, CNCS-UEFISCDI, project number PN-II-ID-PCE-2011-3-0097.

## IV. CONCLUSIONS

In this paper, the MRIP-APSA and its implementation using a fast recursive procedure is proposed. Simulations in the context of network echo cancellation and adaptive feedback control proved that MRIP-APSA obtains superior performances to those of RIP-APSA. The effect of different parameters of the algorithm has been investigated.

## REFERENCES

[1] A.Sayed, Adaptive filters, John Wiley & Sons, 2008.

[2] K. Ozeki and T. Umeda, "An adaptive filtering algorithm using an orthogonal projection to an affine subspace and its properties," Electron. Commun. Jpn., vol. 67-A, no. 5, 1984, pp. 19–27.

[3] M. Bouchard and F. Albu, "The Gauss-Seidel fast affine projection algorithm for multichannel active noise control and sound reproduction systems ", Special Issue on Adaptive Control of Sound

and Vibration, Int. Journal of Adaptive Control and Signal Processing, vol. 19, nr. 2-3, pp. 107-123, March-April 2005.

[4] A. Gonzalez, M. Ferrer, F. Albu and M. de Diego, "Affine projection algorithms: evolution to smart and fast multichannel algorithms and applications", in Proc. of Eusipco 2012, Bucharest, Romania, August 2012, pp. 1965-1969.

[5] F. Albu, C. Paleologu and J. Benesty, "A Variable Step Size Evolutionary Affine Projection Algorithm", in Proc. of ICASSP 2011, Prague, Czech Republic, May 2011, pp. 429-432.

[6] D.L. Duttweiler, "Proportionate normalized least-mean-squares adaptation in echo cancellers", IEEE Trans. Speech Audio Process., vol. 8, no. 5, 2000, pp. 508–518.

[7] J. Benesty and S. L. Gay, "An improved pnlms algorithm," in Proc. of ICASSP 2002, vol. 2, 2002, pp. 1881 –1884.

[8] H. Deng and M. Doroslovacki, "Proportionate adaptive algorithms for network echo cancellation", IEEE Trans. Signal Process., vol. 54, no. 5, 2006, pp. 1794–1803.

[9] O. Hoshuyama, R.A. Goubran and A. Sugiyama, "A generalized proportionate variable step-size algorithm for fast changing acoustic environments," in Proc. of ICASSP 2004, vol. 4, 2004, pp. 161-164.

[10] T. Gansler, J. Benesty, S.L. Gay, and M. Sondhi, "A robust proportionate affine projection algorithm for network echo cancellation," in Proc. of ICASSP 2000, pp. 793–796.

[11] F. Albu, C. Paleologu, J. Benesty, and S. Ciochina, "A low complexity proportionate affine projection algorithm for echo cancellation," in Proc. of EUSIPCO, Aalborg, Denmark, August 2010, pp. 6-10.

[12] J. Yang and G.E. Sobelman, "Efficient $\mu$ -law improved proportionate affine projection algorithm for echo cancellation," Electronics Lett., vol. 47, issue 2, 2010, pp. 73-74.

[13] Y. V. Zakharov, "Low complexity implementation of the affine projection algorithm", IEEE Signal Processing Letters, vol. 15, 2008, pp. 557–560.

[14] F. Albu, "A Proportionate Affine Projection Algorithm using Fast Recursive Filtering and Dichotomous Coordinate Descent Iterations", in Proc. of SPAMEC 2011, Cluj, Romania, pp. 93-96.

[15] F. Albu, H. Coanda, D. Coltuc and M. Rotaru, "Intermittently Updated Simplified Proportionate Affine Projection Algorithm", in Proc. of ADAPTIVE 2014, Venice, Italy, pp. 42-47.

[16] T. Shao, Y.R. Zheng and J. Benesty, "An affine projection sign algorithm robust against impulsive interferences," IEEE Signal Processing Lett., vol. 17, no. 4, 2010, pp. 327–330.

[17] S.J. Ban and S.W. Kim, "Pseudo affine projection sign algorithm for robust system identification," IET Electronics Lett., vol. 46, no. 12 , 2010, pp. 865-866.

[18] Z. Yang, Y. R. Zheng and S. L. Grant, "Proportionate affine projection sign algorithms for network echo cancellation," IEEE Transactions on Audio, Speech, and Language Processing, vol. 19, no. 8, 2011, pp. 2273-2284.

[19] J. Ni, F. Li, "Efficient implementation of the affine projection sign algorithm", IEEE Signal Processing Letters, vol. 19, no. 1, 2012, pp. 24-26.

[20] F. Albu and H.K. Kwan, "Memory Improved Proportionate Affine Projection Sign Algorithm", IET Electronics Letters, vol. 48, (20), October 2012, pp: 1279-1281.

[21] F. Albu and H.K.Kwan, "New proportionate affine projection sign algorithms", in Proc. of ISCAS 2013, Beijing, China, 2013, pp. 1789 – 1793.

[22] T. Waterschoot and M. Moonen, "Fifty years of acoustic echo feedback control: state of the art and future challenges", Proc. IEEE, vol. 99, no. 2, 2011, pp. 288-327.

[23] M. Rotaru, F. Albu and H. Coanda, "A Variable Step Size Modified Decorrelated NLMS Algorithm for Adaptive Feedback Cancellation in Hearing Aids, " in Proc. of ISETC 2012, Timisoara, Romania, 15-16 November 2012, pp. 263-266.

[24] M. Rotaru, C. Stanciu, S. Ciochina, F. Albu and H. Coanda, "A FPGA Implementation of Prediction Error Method for Active Feedback Cancellation using Xilinx System Generator", in Proc. of ADAPTIVE 2013, Valencia, Spain, pp. 26-29.

[25] P. O. Hoyer, "Non-negative matrix factorization with sparseness constraints," J. Mach. Learn. Res., vol. 5, 2004, pp. 1457–1469.

[26] C. R. C. Nakagawa, S. Nordholm, F. Albu, W.-Y. Yan, "Closed-loop feedback cancellation utilizing two microphones and transform domain processing", Proceedings of ICASSP 2014, Florence, Italy, May 2014, pp. 3673-3677.